Available online at www.sciencedirect.com

SCIENCE DIRECT®

Magnetic Resonance Imaging 23 (2005) 215–220

MAGNETIC RESONANCE IMAGING

Modeling diffusion in white matter in the brain: A composite porous medium

Pabitra N. Sen[a,*], Peter J. Basser[b]

[a]Schlumberger-Doll Research, Ridgefield, CT 06877, USA

[b]Laboratory of Integrative & Medical Biophysics, National Institutes of Health (NIH), Bethesda, MD 20892-5772, USA

Abstract

We model diffusion in white matter fascicles as a problem of diffusion in an array of identical thick-walled cylindrical tubes immersed in an outer medium and arranged periodically in a regular lattice. The diffusing molecules have different diffusion coefficients and concentrations (or densities) within the tubes' inner core, membrane, myelin sheath, and within the outer medium. For an impermeable myelin sheath, diffusing molecules within the inner core are completely restricted, while molecules in the outer medium are hindered due to the tortuosity of the array of impenetrable tubes.

Keywords: Diffusion; White matter; Myelin; Axon; Brain; Conductivity; Tensor; Model; MRI

1. Introduction

Diffusion tensor imaging (DTI) is a powerful noninvasive tool to assess developing, normal and pathological white matter in the brain in vivo [1,2]. White matter has an underlying fibrous structure giving rise to an observed anisotropy in the apparent diffusion coefficient (ADC), that is, different ADCs parallel and perpendicular to the fibers. The exact relationship between the apparent diffusion tensor (ADT) and tissue microstructure and composition is not known. In order to probe the dependencies of the ADT on tissue structure and composition, we develop analytical results for the long-time (times much longer than diffusion time across the fibers) ADC and ADT in a simplified model of brain white matter, consisting of a periodic pack of parallel cylindrical permeable multilayered tubes. Specifically, we compute ADCs both parallel and perpendicular to the axis of symmetry as well as the ADT, and relate these quantities to microstructure and compositional parameters.

Recently, Hwang et al. [3] employed the finite-difference method on histological images for simulating restricted diffusion with a view towards assessing neural injury and regeneration in myelinated axons. The literature had been reviewed well by Hwang et al. [3] who stated that the thickness of the myelin sheath had been ignored in all studies prior to theirs. They validated their finite-difference scheme against known analytic solutions for diffusion in a cylindrical pore and in a hexagonal array of cylinders which do not possess thick skins. Specifically, Hwang et al. compared their simulation for cases (a) of a cylindrical pore surrounded by an impermeable medium and (b) hexagonal arrays of permeable cylinders using the results of Perrins et al. [4] for uncoated cylinders. Anatomical sections (Fig. 1) of white matter reveal that the myelin sheath is thick as shown schematically in Fig. 2. To model myelin, we incorporate a finite coating thickness having transport properties represented by myelin's fluid concentration and diffusion coefficient. Numerical studies, such as that by Hwang et al. [3], would benefit from the solutions provided here in which analytical results for the thick-walled tube pack are provided. Below we present results for square and hexagonal packs of coated cylinders that could serve as a test system for validating such numerical calculations.

* Corresponding author.

E-mail address: psen@ridgefield.oilfield.slb.com (P.N. Sen).

0730-725X/$ – see front matter © 2005 Elsevier Inc. All rights reserved.
doi:10.1016/j.mri.2004.11.014

2. Model calculations

Chin et al. [3] concluded that the sensitivity of ADC to difference in T_2 in different compartments is small, allowing us to consider the steady-state diffusion coefficient in a composite media.

Diffusion currents are driven by gradients in the Gibbs chemical potential,

$$\mu = \mu^0 + RT\ln\ C + RT\ln\ a. \tag{1}$$

Here, R is the gas constant, T is the temperature, C is the concentration of the substance that is diffusing, a is the activity coefficient, and μ^0 is the chemical potential of the substance in its standard state. μ^0 is independent of position; we will assume either the substance is ideal ($\ln a \equiv 0$) or $\ln a$ does not vary with position, and the temperature is uniform throughout. To be explicit, the particle current density is given by the constitutive relation

$$\begin{aligned} j(\mathbf{r}) &= -\tfrac{D}{RT} C(\mathbf{r}) \nabla \mu(\mathbf{r}) \\ &= -D \nabla C(\mathbf{r}). \end{aligned} \tag{2}$$

We use the analogy between Eq. (2) and the corresponding constitutive relations between electric currents (displacement or conduction) and electric potential gradient via dielectric constant or electrical conductivity. We can apply the solutions for electrical conductivity or dielectric constants for composite media made up of coated cylinders [5,6] by replacing the electrical potential, $V(r, \theta)$, by a chemical potential $\mu\ (r, \theta) = \mu^0 + RT\ \ln[C(r, \theta)]$ (we lump position-independent $RT\ \ln\ a$ with μ^0). For the corresponding diffusion problem, the conductivities or dielectric constants of each region are replaced by the product of the diffusion coefficient and the concentration of the corresponding region. The additional factor of concentration plays an important role in the tortuosity factor of the effective diffusion coefficient [7,8].

We use a subscript "c" to denote the core, "s" to denote the sheath and "b" to denote extra-axonal (bath) material. The equilibrium concentration and diffusion coefficients of the molecules under investigation inside the core are C_{c0} and D_c, those inside the myelin sheath are C_{s0} and D_s, and those outside are C_{b0} and D_b. Note that in Eq. (1), $C_c(\mathbf{r}) = C(r, \theta)$, etc., denotes perturbations to the equilibrium concentrations C_{c0}, etc., due to an externally imposed concentration or chemical potential gradient, which can be likened to an electric field, E_{ext}, that is used in the corresponding problem of electrical conductivity or dielectric constant of composite media [4–6].

We consider both a square pack and a hexagonal pack of cylinders (Fig. 3). In both the cases, the cylinder centers are separated by a distance L, the radius of the inner cylinder is r_c and that of the outer is r_s, and thus the sheath thickness is given by $\Delta t = r_s - r_c$. Only the ratios of these lengths will appear in the answer.

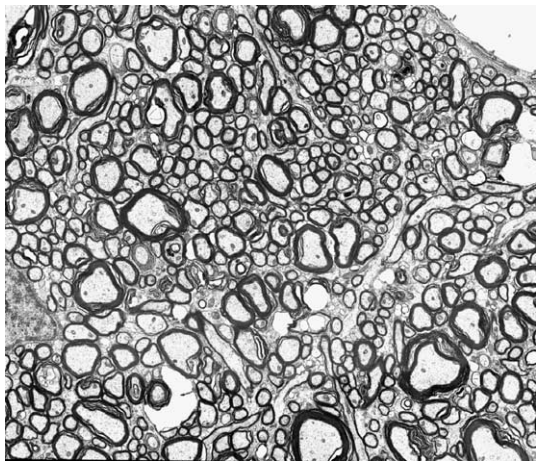

Fig. 1. Histology showing bundles of axons in a section of primate white matter (cross section of corpus callosum). Water diffuses faster parallel to the fibers than perpendicular to them.

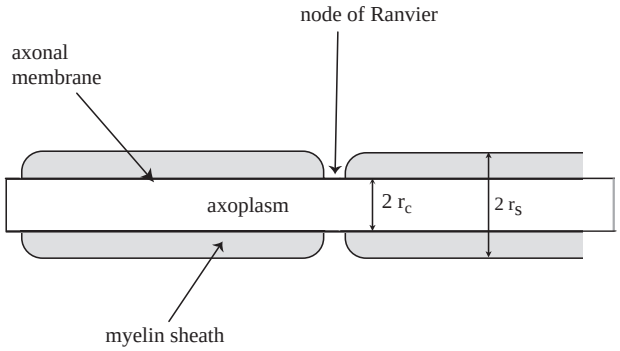

Fig. 2. A schematic diagram of a myelinated axon. The axonal membrane contains short active regions, nodes of Ranvier, which are joined by long passive segments insulated by myelin. The outer radius of the axon is r_s; its inner radius r_c.

Mathematical details will be presented elsewhere. The effective concentration C_{eff} is:

$$C_{\text{eff}} = (1-f)C_{\text{b0}} + f\frac{r_c^2}{r_s^2}C_{\text{c0}} + f\left(1-\frac{r_c^2}{r_s^2}\right)C_{\text{s0}}. \tag{3}$$

The effective properties for coated cylinders depend on geometrical structure factors [4–6] and factors γ_{2l-1} that depend on the properties of the constituents:

$$\gamma 2l-1 = \frac{(D_{\text{b}}C_{\text{b0}} - D_{\text{s}}C_{\text{s0}})(D_{\text{s}}C_{\text{s0}} - D_{\text{c}}C_{\text{c0}})r_c^{2(2l-1)} + (D_{\text{b}}C_{\text{b0}} + D_{\text{s}}C_{\text{s0}})(D_{\text{c}}C_{\text{c0}} + D_{\text{s}}C_{\text{s0}})r_s^{2(2l-1)}}{(D_{\text{b}}C_{\text{b0}} + D_{\text{s}}C_{\text{s0}})(D_{\text{s}}C_{\text{s0}} - D_{\text{c}}C_{\text{c0}})r_c^{2(2l-1)} + (D_{\text{b}}C_{\text{b0}} - D_{\text{s}}C_{\text{s0}})(D_{\text{c}}C_{\text{c0}} + D_{\text{s}}C_{\text{s0}})r_s^{2(2l-1)}}. \tag{4}$$

The longitudinal effective diffusion coefficient $D_{\text{l,eff}}$ is given by the volume averages:

$$D_{\text{l,eff}}C_{\text{eff}} = (1-f)D_{\text{b}}C_{\text{b0}} + f\frac{r_c^2}{r_s^2}D_{\text{c}}C_{\text{c0}} + f\left(1-\frac{r_c^2}{r_s^2}\right)D_{\text{s}}C_{\text{s0}}, \tag{5}$$

for all packing geometries.

A reasonable measure of diffusion anisotropy can be given by the ratio $D_{\text{l,eff}}/D_{\text{t,eff}}$, and this ratio is independent of C_{eff}. <ADC>, the mean ADC, and the degree of anisotropy, $D_{\text{l,eff}}/D_{\text{t,eff}}$, are two useful parameters routinely used in characterizing white matter.

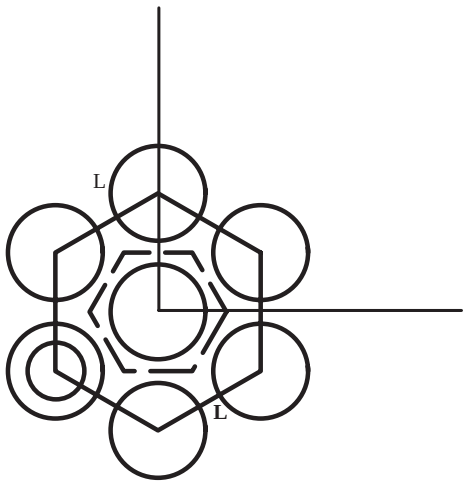

Fig. 3. Nearest neighbors around the central cylinder of a portion of a hexagonal array of coated cylinders. To remove clutter, only one cylinder is depicted as coated; only the outer radius is shown for the others. Centers of cylinders are separated by a distance L, hence $f = \frac{2}{\sqrt{3}}\frac{\pi r_s^2}{L^2}$, where r_s is the outer radius.

In square and hexagonally symmetric packs, the symmetry dictates that the diffusion tensor be described by two principal diffusion coefficients—one parallel to the axis of the cylinders and the other perpendicular to it, lying in the transverse plane (i.e., diffusion is isotropic in the transverse plane and two transverse components of the tensor are identical).

For a square array, $f=\pi r_s^2/L^2$ is the fraction of volume occupied by the coated cylinders. To the lowest order in multipolar concentration, we obtain the Maxwell-Garnett formula:

$$D_{t,eff}C_{eff} = D_bC_{b0}\left[1-\frac{2f}{\gamma_1+f}\right]. \tag{6}$$

A truncation to third order gives,

$$D_{t,eff}C_{eff} = D_bC_{b0}\left[1-2f\left(\gamma_1+f-\frac{0.305828f^4\gamma_5}{\gamma_3\gamma_5-1.402960f^8}\right)^{-1}\right] \tag{7}$$

While for the square lattice geometry, the maximum value of f is $\pi/4 \approx 0.785$, published values of the intracellular space based on iontophoretic measurements are typically higher, approximately 0.82. In order to treat the physiological range of axon spacing, we must consider hexagonal (and possibly other) packing geometries that afford higher packing densities.

For a hexagonal array,

$$f = \frac{2\pi r_s^2}{\sqrt{3}L^2}. \tag{8}$$

Thus, the maximum packing density is about $f=0.907$. To the lowest order in multipolar expansion, we obtain again the Maxwell-Garnett formula, Eq. (6), which is the same as that for a square array. In fact, the Maxwell-Garnett formula holds for all structures, including for disordered systems and is accurate for small f, that is, in the dilute limit. Next, the same degree of truncation in recursion relations as employed in Eq. (7) gives for hexagonal pack:

$$D_{t,eff}C_{eff} = D_bC_{b0}\left[1-2f\left(\gamma_1+f-\frac{0.07542f^6\gamma_7}{\gamma_5\gamma_7-1.06028f^{12}}\right)^{-1}\right] \tag{9}$$

In the absence of a sheath, we recover Eq. (13) of Perrins et al. [4].

In the usual permeability approximation, one takes the limit of thin skin such that $\Delta t=r_s-r_c\to 0$ with $D_s/(\Delta t)\to\kappa$, giving a jump condition.

All the results for longitudinal and transverse diffusion coefficients are easily generalized for the thin myelin case by the use of an appropriate limit.

A thick myelin sheath is nearly impermeable and acts as a diffusion barrier. For the nearly impermeable myelin case, the effective transverse diffusion coefficient times the effective concentration $D_{t,eff}C_{eff}$ does not depend on properties of the core. This is intuitively obvious: if the diffusion in the sheath is practically zero, it acts as a barrier and $D_{t,eff}C_{eff}$ is dominated by diffusion outside the sheath. The core contribution then drops out (is shielded out); however, the effective concentration C_{eff} involves the properties of the core.

In the extreme limit, when $C_cD_c=C_sD_s=0$, all transport comes from the bath molecules, but they have a tortuous path to follow in the transverse direction. The Maxwell-Garnett form for transverse diffusivity is $D_{t,eff}=D_b/(1+f)$, whereas $D_{l,eff}=D_b$.

In this case of no myelin, one can use the results from Perrins et al. [4] of uncoated cylinders. The diffusion tensor can still be anisotropic, even in the absence of a myelin sheath. Let us illustrate this using the lowest order of the so-called Maxwell-Garnett form, Eq. (6), for transverse diffusivity:

$$\frac{D_{l,eff}}{D_{t,eff}} = \frac{(C_bD_b(1-f)+C_cD_cf)(C_cD_c(1-f)+C_bD_b(1+f))}{C_bD_b(C_bD_b(1-f)+C_cD_c(1+f))}$$

Note that in Eq. (10) above, the anisotropy vanishes when $C_bD_b=C_cD_c$, but the system will be anisotropic even when $D_b=D_c$, but $C_b\neq C_c$.

3. Results and discussions

Analytical solutions for the ADT and quantities derived from it, such as the mean ADC, <ADC>, and the degree of diffusion anisotropy, can be used to explore the effects of small changes in model parameters associated with normal conditions as well as a number of developmental and disease processes known to affect myelinated axon structure and function.

Many studies suggest the existence of diffusion anisotropy in white matter prior to the appearance of myelin [9,10]. That there can be anisotropy even in the absence of a myelin sheath is obvious. For example, when cylinders with high values of $C_c D_c$ (containing highly diffusive molecules) are inserted in a bath with small values of $C_b D_b$ (containing poorly diffusive molecules), the longitudinal transport can be high; while the transport perpendicular to the cylinder axes will be low, as the molecules within the cylinders have to diffuse through the bath in the transverse direction but not in the longitudinal direction. This phenomenon can be likened to resistors in series (transverse direction) and resistors in parallel (longitudinal direction).

When present, myelin is the major barrier to diffusion and cause of anisotropy. In normal white matter development, the thickness of the myelin sheath increases. We can mimic this process heuristically by considering the case in which the normalized thickness of the myelin sheath, $(r_s - r_c)/r_c$, grows from zero to a finite value. Fig. 4 shows the mean <ADC> as a function of the radius of the myelin sheath. As myelin thickness increases, the mean ADC progressively drops, a change that is in qualitative agreement with the findings of Neil et al. [9]. In Fig. 5, the anisotropy ratio is plotted vs. the radius of the myelin sheath. Some diffusion anisotropy is observed when no myelin is present, but the fact that anisotropy increases with increasing myelin thickness supports the hypothesis that, although not the only determinant of diffusion anisotropy in white matter, myelin can significantly contribute to it.

In DT-MRI, one measures an attenuation in the magnetization due to random phases that the spins acquire during its random motion. In the lowest order of approximation, the attenuation exponent depends on the mean square displacement. Here, we have considered only the long-time limit of diffusion coefficient, which is the mean square displacement divided by time. For hindered motion or permeable myelin, one can use the diffusion coefficient times time to recover the mean square displacement. However, for fully restricted motion of axonal fluid molecules, as in the case of an impermeable myelin, the mean square displacement is bounded, and the long-time diffusion coefficient of restricted axonal fluid molecules becomes zero. Thus, the mean square displacement is nonrecoverable from the long-time diffusion coefficient. The implications for DT-MRI have been studied in a recent paper [11]. To characterize water diffusion in brain white matter, Assaf et al. [11] proposed a framework that incorporates both hindered and restricted models of water diffusion and an experimental methodology that embodies features of diffusion tensor and q-space MRI. They propose a model of white matter diffusion anisotropy that contains a hindered extra-axonal compartment, whose diffusion properties are characterized by an effective diffusion tensor, and an intra-axonal compartment, whose diffusion properties are characterized by a restricted model of diffusion within cylinders. The hindered model primarily explains the Gaussian signal attenuation behavior observed at low b (or q) values; the restricted non-Gaussian model does so at high b (or q).

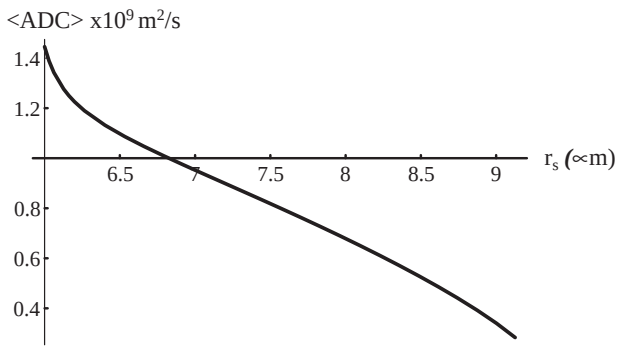

Fig. 4. Mean diffusion coefficient$\langle ADC\rangle = \left(2D_{t,\mathrm{eff}} + D_{l,\mathrm{eff}}\right)/3$ as a function of the myelin sheath radius r_s develops from its minimum value of r_c to that allowed by hexagonal close pack. Here, $r_c = 6$ μm, $D_b = 2\times10^{-9}$ m^2/s, $C_{b0} = 0.95$, $D_c = 7.5\times10^{-10}$ m^2/s, $C_{c0} = 0.88$, $D_s = 3.\times10^{-11}$ m^2/s, $C_{s0} = 0.5$, and $L = 18.2$ μm.

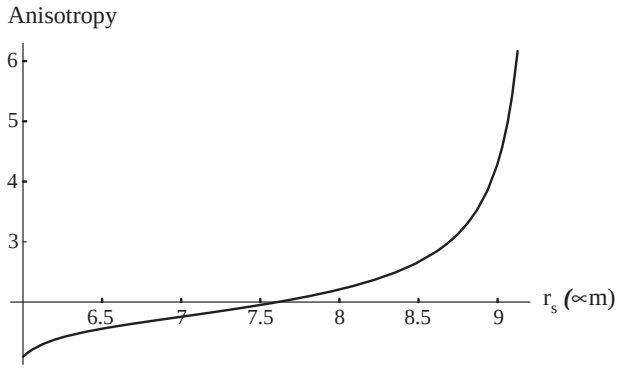

Fig. 5. Degree of diffusion anisotropy $D_{l,\mathrm{eff}}/D_{t,\mathrm{eff}}$ as a function of the myelin sheath radius r_s develops from its minimum value of r_c to that allowed by hexagonal close pack. Here, $r_c = 6$ μm, $D_b = 2\times10^{-9}$ m^2/s, $C_{b0} = 0.95$, $D_c = 7.5\times10^{-10}$ m^2/s, $C_{c0} = 0.88$, $D_s = 3.\times10^{-11}$ m^2/s, $C_{s0} = 0.5$, and $L = 18.2$ μm.

4. Conclusion

Here, we have presented a simplified, but self-consistent modeling framework for predicting the long-time ADCs of water parallel and perpendicular to a pack of myelinated axons. Values assumed for white matter suggest that the orientationally averaged ADC (mean ADC) and diffusion anisotropy ratio are fairly insensitive to intracellular dimensions and diffusion properties, and are primarily

affected by changes in the outer diameter of the axons, the extracellular volume fraction, and inter-axonal spacing.

References

[1] Basser PJ, Pajevic S, Pierpaoli C, Duda J, Aldroubi A. In vivo fiber tractography using DT-MRI data. Magn Reson Med 2000;44: 625–32.

[2] Pierpaoli C, Jezzard P, Basser PJ, Barnett A, Di Chiro G. Diffusion tensor MR imaging of the human brain. Cardiovasc Radiol 1996;201: 637–48.

[3] Hwang SN, Chin C-L, Wehrli FW, Hackney DB. Image-based finite difference model for simulating restricted diffusion. Magn Reson Med 2003;50:373–82.

[4] Perrins WT, McKenzie DR, McPhedran RC. Proc R Soc Lond A 1979;369:207.

[5] Nicorovici NA, McPhedran RC, Milton GW. Transport properties of a three-phase composite material: the square array of coated cylinders. Proc R Soc Lond 1993;442:599–620.

[6] Nicorovici NA, McKenzie DR, McPhedran RC. Optical resonances of three-phase composites and anomalies in transmission. Opt Commun 1995;117:151–69.

[7] Johnson DL, Sen PN. The multiple scattering of acoustic waves with application to the index of refraction of 4th sound. Phys Rev 1981; B24:2486.

[8] Mair RW, Hürlimann MD, Sen PN, Schwartz LM, Patz S, Walsworth RL. Tortuosity measurement and the effects of finite pulse widths on xenon gas diffusion NMR studies of porous media. Magn Reson Imaging 2001;19:345–51.

[9] Neil JJ, Shiran SI, McKinstry RC, Schefft GL, Snyder AZ, Almli CR, et al. Normal brain in human newborns: apparent diffusion coefficient and diffusion anisotropy measured by using diffusion tensor MR imaging. Radiology 1998;209:57–66.

[10] Neil J, Miller J, Mukherjee P, Huppi PS. Diffusion tensor imaging of normal and injured developing human brain - a technical review. NMR Biomed 2002;15:543–52.

[11] Assaf Y, Freidlin RZ, Rohde GK, Basser PJ. New modeling and experimental framework to characterize hindered and restricted water diffusion in brain white matter. Magn Reson Med 2004;52:965–78.